



Comparison of precipitation measurements by Ott Parsivel² and Thies LPM optical disdrometers

Marta Angulo-Martínez¹, Santiago Beguería¹, Borja Latorre¹, and María Fernández-Raga²

¹Experimental Station of Aula Dei, Consejo Superior de Investigaciones Científicas (EEAD-CSIC), Avda. Montañana 1005, Zaragoza, E-50059, Spain

²Dept. of Physics, University of Leon, Spain

Correspondence to: M. Angulo-Martínez (marta.angulo@eead.csic.es)

Abstract.

Optical disdrometers are present weather sensors with the ability of providing detailed information of precipitation such as rain intensity, kinetic energy or radar reflectivity, together with discrete information on the distribution of particle sizes and fall velocities (PSVD) of the hydrometeors. Disdrometers constitute a step forward towards a more complete characterisation of precipitation, being highly useful in several research fields and applications. In this article the performance of the two optical disdrometer most extensively used, the most recent version of Ott PARSIVEL² disdrometer and Thies Clima Laser Precipitation Monitor, is evaluated. During a two years precipitation observation experiment, four collocated optical disdrometers, two Thies Clima LPM and two Ott PARSIVEL², recorded 58761 common one-minute precipitation observations, totalling 221 natural rainfall events, with intensities peaking at 220 mm h⁻¹. The results show significant differences between both disdrometer types for all integrated precipitation parameters, which can be explained by differences in the raw particle size and velocity distribution (PSVD). Thies LPM recorded in average double number of particles than PARSIVEL². PSVD percentile comparison showed Thies LPM measuring more small particles than Ott Parsivel², resulting in higher rain rates and totals. These differences increased greatly with rainfall intensity. At rain rates above 10 mm h⁻¹ Thies LPM recorded nine times the number of particles of PARSIVEL², affecting all precipitation variables. The practical consequences of these differences, and possible reasons, are discussed, in order to help researchers and users in the election of the sensor, pointing out at the same time limitations to be fixed in future versions.



1 Introduction

Disdrometers are devices designed to measure the particles size distribution (PSD), or size and velocity distribution (PSVD), of falling hydro-meteors. The PSD describes the statistical distribution of falling particle sizes from the number of particles with a given equivolume diameter per unit volume of air. The PSVD includes also information about the distribution of the particles fall velocities.

Information on the PSD / PSVD is required for a proper understanding of hydrometeorological regimes (Iguchi et al., 2000; Krajewski et al., 2006; Adirosi et al., 2016; Angulo-Martínez and Barros, 2015), soil erosion (Sempere-Torres et al., 1998; Loik et al., 2004; Cruse et al., 2006; Petan et al., 2010; Fernández-Raga et al., 2010; Shuttleworth, 2012; Iserloh et al., 2013; Angulo-Martínez et al., 2016) and other applications such as pollution wash off in urban environments (Kathiravelu et al., 2016; Castro et al., 2010).

Rainfall estimation by remote sensing, radar and satellite, also rely on PSD information (Olsen et al., 1978; Atlas et al., 1999; Uijlenhoet and Sempere, 2006; Tapiador et al., 2017). Disdrometers are also widely used to validate the reflectivity values obtained by weather radars, for what the studies on small scale PSD spatio-temporal variation and its influence in modeling PSD and rainfall rate - reflectivity ($Z(R)$) relations are particularly important (Krajewski et al., 1998; Löffler-Mang and Blahak, 2001; Miriovsky et al., 2004; Thurai and Bringi, 2008; Marzano et al., 2010; Jaffrain and Berne, 2012; Jameson et al., 2015; Raupach and Berne, 2016; Gires et al., 2016). Many of these studies took place within Precipitation Measurement Missions helping developing better sensors and algorithms for precipitation detection and quantification; some examples are: Ioannidou et al. (2016) for the Tropical Rainfall Measurement Mission (TRMM), Liao et al. (2014) and Tan et al. (2016) for the Global Precipitation Measurement Mission (GPM), Adirosi et al. (2016) for the Hydrological cycle in the Mediterranean Experiment (HyMex), or Calheiros and Machado (2014) for the CHUVA campaign. In addition, bulk precipitation variables, such as rain rate, liquid water content, radar reflectivity or rainfall kinetic energy, among others, can also be calculated from PSD moments (Ulbrich, 1983; Testud et al., 2001; Jameson and Kostinski, 1998), and as such disdrometers have been incorporated in operational meteorological networks as present weather sensors and pluviometers.

Current commercial disdrometers are based mainly in two physical principles to measure the PSD. The first ones are electro-mechanical impact devices recording the electrical pulses produced by the pressure of falling drops when impacting over a surface. Impact disdrometers such as the Joss and Waldvogel disdrometer (JWD), (Joss and Waldvogel, 1967) or piezoelectric force transducers (Jayawardena and Rezaur, 2000) were largely used in the 1980s and 90s. The JWD disdrometer gives good results for light to moderate intensity but underestimates the amount of small size drops during heavy rainfall events, and it cannot detect raindrops smaller than 0.3 mm of diameter (Tokay et al., 2001). Pressure disdrometers, however, can only measure the PSD, and the velocity of the meteors is inferred based on theoretical terminal velocity models. More recent disdrometers are based in optical principles (Löffler-Mang and Joss, 2000), either from the occlusion of a laser light beam between an emisor and a receptor device produced by the particle passing through; or based on light scattering measurements



from particles passing through the light beam. Both types use an emissary and a receiver of the laser signal generally in a horizontal plane, and the emissary can be punctual or an array of emissaries. Commercial examples of the first type are the particle size and velocity disdrometer PARSIVEL and PARSIVEL² by Ott Hydromet, and the Laser Precipitation Monitor LPM by Thies Clima. An example of the light scattering principle is the light scatter sensor PWS100 (Campbell Scientific Inc.). Optical disdrometers provide full PSVD measures from the unique light beam horizontal plane (~1 cm thick) by the amplitude and duration obscuration when particles pass through the beam, respectively. Laser disdrometers are not devoid of detection problems related with the effect of wind, splashing, oscillations in the laser current and temperature, multiple drops appearing at the same time, margin-fallers resulting in partial detections, and others (Tokay et al., 2001; Kruger and Krajewski, 2002; Frasson et al., 2011; Raupach and Berne, 2015). An improvement over laser disdrometers is the two-dimensional video disdrometer (2DVD, Joanneum Research). The 2DVD uses two perpendicular high-speed line-scan cameras, each with an opposing light source, to measure particles from orthogonal angles. The 2DVD provides reliable measures of particles fall velocity, size and shape (Kruger and Krajewski, 2002). Currently this disdrometer provides is considered as the most accurate PSVD measurements of particles from 0.3 mm of diameter, although its use is mostly restricted to experimentation due to its higher cost and data processing requirements.

A bibliography search by the key phrase "optical AND disdrometer" on publications between 2000 and 2017 in Scopus showed that the two models most currently used are Ott PARSIVEL (mentioned in 50% of a total of 200 documents) and Thies LPM (mentioned in 25%). In some disciplines, both disdrometers have been used interchangeably. This is the case, for instance, of soil erosion studies, where Thies LPM was used for monitoring rainfall characteristics, most notably the kinetic energy, in relation with splash erosion experiments (Angulo-Martínez et al., 2012; Fernández-Raga et al., 2010), and also in the calibration of the European portable rainfall simulator (Iserloh et al., 2013). PARSIVEL disdrometers, on the other hand, have been used to determine the kinetic energy - rainfall intensity relationship (Petan et al., 2010; Sanchez-Moreno et al., 2012). Both disdrometers were used indifferently in Slovenia to estimate rainfall parameters, including kinetic energy (Petan et al., 2010; Ciaccioni et al., 2016), and to inter-compare solid precipitation observations in the Tibetan Plateau (Zhang et al., 2015).

The performance of Parsivel and Thies disdrometers has been evaluated by comparison with more accurate disdrometers such as the 2DVD, the JWD, or by taking a pluviometer as a reference. PARSIVEL disdrometers have been evaluated since its first version became commercially available from PM Tech Inc (Sheppard and Joe, 1994). Several versions of this device have been used for disdrometer evaluation and precipitation comparisons through time, with the results obtained linked to the purchased PARSIVEL version of the time, with its drawbacks (Krajewski et al., 2006; Lanza and Vuerich, 2009; Battaglia et al., 2010; Jaffrain and Berne, 2011; Thurai et al., 2011; Park et al., 2017). In 2005, Ott Hydromet purchased the rights of PARSIVEL disdrometer and redesigned the instrument. Differences between the PM Tech (P0) and the first version of Ott Hydromet PARSIVEL (P1) are described in Tokay et al. (2013). In 2011, Ott Hydromet redesigned P1 and made available Ott PARSIVEL² (P2). This new PARSIVEL version included a more expensive and homogeneous laser beam and some other modifications that improve its performance (Tokay et al., 2013, 2014; Angulo-Martínez and Barros, 2015). The current version of Ott PARSIVEL² (P2) is the best PARSIVEL version commercially available, as it has been explained by Tokay et al. (2014).



The P2 has been compared with other accurate disdrometers such as the JWD and the 2DVD (Tokay et al., 2013, 2014; Raupach and Berne, 2015; Park et al., 2017). Thies LPM, on the other hand, became commercially available in 2005 from Adolf Thies GmbH & Co. The first evaluation of the sensor, in terms of rain rate and amount, was presented by Lazinger et al. (2006) at the WMO Technical Conference on Meteorological and Environmental instruments and methods of observations (TECO-2006).
5 Since then, this type of disdrometer has been used worldwide with several firmware updates. The Thies LPM performance was thoroughly analyzed later by Frasson et al. (2011).

To our knowledge, however, only the works of Brawn and Upton (2008) and Upton and Brawn (2008) inter-compared the performance of Thies and PARSIVEL disdrometers in terms of the PSVD and precipitation bulk variables, as well as in terms of the fitted gamma distribution parameters. In their studies they used data from an older PARSIVEL version, and no study
10 up to date has focused on comparing the Thies LPM and the PARSIVEL² devices. Such a study, however, is highly needed if conclusions drawn from measurements made with these two disdrometers want to be compared.

This study aims at comparing the measurements recorded by Thies LPM and most recent Ott PARSIVEL² commercial optical disdrometers, with the objective of providing a quantitative assessment of both sensors and highlighting the associated uncertainties. Measurements of PSVD and integrated rainfall variables as rain rate, kinetic energy, reflectivity and number of drops
15 per volume of air under natural rainfall events are compared, either at the one-minute, the event and the season scales. Some technical problems that arise from the different binning of the PSVD matrix by the two devices, which hinder the comparison between their measurements, are dealt with. In the following section a description of the sensors and the sampling site is given, together with details of the data processing. Section 3 analyses the results obtained, which are discussed in section 4. Section 5 concludes.

20 2 Data and Methods

2.1 Sampling site and instrumentation

Rainfall characteristics under natural conditions were monitored at Aula Dei Experimental Station (EEAD-CSIC) in the central Ebro valley, NE Spain (41°43'30"N, 0°48'39"W, 230 m.a.s.l.). The experimental site is classified as having a cold semiarid climate (BSk, Köppen). Average annual precipitation is 315 mm with equinoctial rainfalls, which are usually more intense
25 during fall.

Four disdrometers, two Thies Clima LPM and two Ott PARSIVEL², were operated in continuous record during the period between 17/06/2013 and 21/07/2015. Two disdrometers of every type were placed in two masts (Mast-1 and Mast-2), which were located 1.5 m apart from each other (Figure 1). Each mast consisted in a pole with two arms 0.5 m apart from each other where two devices, one of each model, were installed. One-minute rainfall DSD observations were recorded automatically



during the period, and rainfall episodes were identified according to the following criteria: a rainfall episode started when rainfall was continuously recorded by at least two disdrometers of different type during at least 10 minutes; and two rainfall episodes were delimited by, at least, one entire hour without rain in by at least two disdrometers of different type.

[FIGURE 1: Sampling site with four collocated disdrometers]

5 Both optical disdrometers, Thies Clima LPM and Ott PARSIVEL², are based on the same measurement principle. Their external structure is formed by two heads that connect the sheet of laser light through which falling drops are measured. Drop diameter and fall velocity are determined from the obscurations amplitude and duration in the path of an infrared laser beam, between a light emitting diode and a receiver, within a sampling area of approximately 0.005 m², with slight deviations depending on the sensor (Donnadieu et al., 1969; Löffler-Mang and Joss, 2000). The geometry of the beam limits the estimation
10 of fall velocity to the vertical component (Salles et al., 1999), producing biased measures when the particles fall with a different trajectory or angle due to wind or eddy drag. Correct measurements are also limited to one input point, so other source of biased measurements is due to the co-occurrence of simultaneous drops, which are perceived as just one single drop by the sensor. Similarly, the event of one drop falling on the border of the laser beam ("margin faller"), therefore being only partially observed, leads to biased measurements. The laser signal is then processed by a proprietary software, and the PSVD matrix
15 counting the number of drops for given size and velocity classes, together with several integrated variables, are outputted at regular time intervals (usually one-minute).

Apart from hardware differences, i.e. type of laser and instrument design, the variables and data from each sensor barely differ from one another. Raindrops are assumed spherical for sizes less than 1 mm in diameter, and therefore the size parameter is the equivalent diameter for raindrops below this size. For larger raindrops, a correction for oblateness is made. Both sensors
20 mention in their manuals some correction for edge-detection (particles that are partially measured at the edge of the laser beam) and coincident particles passing at the same time through the laser beam, although there is no information on how these two events are identified and treated. The main initial difference between the two disdrometer types is in how they store particles by size and velocity. More details of both instruments and the measurement technique, along with the assumptions used to determine the size and velocity of hydrometeors, can be found in Löffler-Mang and Joss (2000); Battaglia et al. (2010);
25 Tapiador et al. (2010); Frasson et al. (2011); Jaffrain and Berne (2011); Tokay et al. (2013, 2014); Raupach and Berne (2015), and in their respective technical manuals.

Thies Clima Laser Precipitation Monitor

The Laser Precipitation Monitor (LPM) measures the size (diameter) and fall velocity of every raindrop greater than 0.12 mm of diameter. It measures precipitation starting from intensities of 0.001 mm h⁻¹. Drop diameters and velocities are grouped into
30 22 and 20 classes ranging between 0.125 mm up to 9 mm and 0 m s⁻¹ up to 12 m s⁻¹, respectively (Table 1). The laser beam



is 228 mm long, 20 mm wide, and 0.75 mm thick on average, and the geometric deviations from the standard are reported by the manufacturer. From these data several rainfall variables are integrated internally by the device's firmware. In this study we focused on rainfall intensity (R , mm h^{-1}), rainfall amount (P , mm), total number of particles (NP), and radar reflectivity (Z , $\text{dB mm}^6\text{m}^{-3}$). In addition, several sensor status and measurement quality variables are provided in the data telegrams informing about voltage oscillations, sensor temperature, and other issues. Rainfall kinetic energy (E , $\text{J m}^{-2} \text{mm}^{-1}$, and Ke , J m^{-2}) is an interesting bulk variable because it combines PSVD with rainfall intensity, informing on the rainfall impact force. The Thies LPM does not provide this variable, so it was calculated from the PSVD as follows: first, total kinetic energy ke_{sum} per minute was determined by multiplying the kinetic energy of every drop belonging to every diameter and velocity bin by the number of drops registered in each size and velocity class. Then, the rainfall kinetic energy per unit surface and precipitation amount was obtained by dividing by the sampling area of the device (in our case, $a_{Thies1} = 0.00467 \text{ m}^2$, and $a_{Thies2} = 0.00490 \text{ m}^2$) and by rainfall amount per minute (P_r):

$$KE = \frac{ke_{sum}}{aP_r} = \frac{\sum N \frac{1}{12} 10^{-3} \pi \rho v_j^2 D_i^3}{aP_r} \quad (1)$$

where N is the number of drops recorded by size and velocity class; D_i is the mean diameter for class i (mm); ρ is the density of water (1 g cm^{-3}); and v_j is the mean speed for the velocity class j in (m s^{-1}).

15 Ott PARSIVEL² disdrometer

The PARSIVEL disdrometers used in this study belong to the second generation manufactured by Ott Hydromet Inc, which include several improvements in PSVD determination in comparison with the previous generation (Tokay et al., 2014; Angulo-Martínez and Barros, 2015; Raupach and Berne, 2015; Park et al., 2017). The measured particles are stored in drop diameter and fall velocity bins in a 32×32 matrix with uneven intervals starting at 0.25 mm diameter up to 25 mm and from 0.05 m s^{-1} up to 20 m s^{-1} (Table 1). The first two size categories, which correspond to sizes of less than 0.2 mm, have been left empty by the manufacturer because of the low signal-to-noise ratio. PARSIVEL² disdrometers detect raindrops from 0.25 mm of diameter. The minimum precipitation rate is 0.007 mm h^{-1} . The PARSIVEL laser beam is 180 mm long, 30 mm wide, and 1 mm thick on average, with no indication about deviations from these values from the manufacturer. The sampling area for all PARSIVEL disdrometers is thus 0.0054 m^2 .

25 PARSIVEL² disdrometers external structure differs from the Thies LPM in incorporating a splash protection shield above the laser heads, which aims at minimizing the effect of splashed drops that interfere with a high velocity with the laser beam and result in biased measurements. Integrated variables from PARSIVEL disdrometer include the internal calculation of rainfall kinetic energy.



[TABLE 1]

2.2 Processing disdrometer data

One minute disdrometer data telegrams were stored in an industrial PC (Matrix 504 Artilla Inc). The PC included specific software to collect, pre-process and send data telegrams to a central server. Time synchronisation was performed once per
5 day using the Network Time Protocol (NTP), allowing bias correction of the internal disdrometer clocks that have a tendency to drift. Minimal processing resulted in one-minute complete time series for the full observation period which included the variables of interest, an error code, and the particles diameter and velocity percentiles (Table 2).

[TABLE 2]

As shown in Table 1, Thies LPM and Ott PARSIVEL² store the number of particles identified in a matrix classified, by size
10 and velocity, in bins which differ in their length and in the minimum and maximum values. In order to compare PSVD data between disdrometer types, particle size and velocity percentiles were calculated. One problem that arises when percentiles are computed from binned data is that the resulting percentiles may be biased depending on the binning structure of the data. If all the particles recorded in one bin are assigned the mean value of the bin (the easiest option), different bin configurations will lead to different computed percentiles, even if the raw data before binning were the identical. When data from different
15 binning structures are compared, as it is the case here between Thies and PARSIVEL disdrometers, an interpolation scheme needs to be used for distributing the range of values within each bin across all the particles corresponding to that bin. Here we used a random distribution over the range of values in the bin following a linear probability distribution constructed by fitting a line between two points determined as the average of the number of particles in the bin and the corresponding values on the neighbouring bins. Once all the number of particles by minute were assigned particle size and velocity values, the percentiles
20 were calculated, allowing for a comparison between disdrometers.

In this study we compare both disdrometer types primary bulk (integrated) variables obtained directly from the telegram itself and, in addition, we do the same comparison calculating all bulk variables after a filter, considering only particles equal or greater than 0.3 mm of diameter, was applied to the data. Due to the low signal-to noise ratio Ott PARSIVEL² start measuring particles from 0.25 mm of diameter. Disdrometers as 2DVD or JWD do not consider drops smaller than 0.3 mm of diameter,
25 therefore we also compared both disdrometer types bulk variables and PSVD percentiles calculated once particles smaller than 0.3 mm of diameter were discarded. Only common minutes of precipitation recording at least 0.1 mm h⁻¹ and more than 10 particles in all disdrometers, were considered.

All data processing, including reading the raw telegrams, computing the integrated variables (erosivity for Thies LPM and size and velocity percentiles), and plOting, was performed using a custom package for the R environment, `disdRo` (Beguería
30 et al., 2017).



2.3 Comparison of disdrometer measurements

The variables listed in Table 2 were compared between the four sensors. A Gamma generalised linear mixed model (Gamma GLMM) was used to compare between disdrometer types. A Gamma distribution was used to model the dependent variable, since this distribution is best suited to positive data with variance increasing with the mean, as it is the case of the disdrometric variables analysed here. Mixed models allow incorporating both fixed-effects and random-effects in the regression analysis (Pinheiro and Bates, 2000). The fixed-effects describe the values of the response variable in terms of explanatory variables that are considered to be non-random, whereas random-effects are treated as arising from random causes, such as those associated with individual experimental units sampled from the population. Hence, mixed models are particularly suited to experimental settings where measurements are made on groups of related, and possibly nested, experimental units. If the classification factor was ignored when modelling grouped data, the random (group) effects would be incorporated to the error term, leading to an inflated estimate of within-group variability. In our case, differences on the response variables (Table 2) were examined considering the disdrometer type as the fixed effect. In order to account for possible differences between measurements unrelated to the disdrometer type but arising from random spatial differences in the rainfall characteristics, a location random effect (the mast to which each disdrometer was attached) was also incorporated in the model. Thus, two independent measurements (replicates) were available for each disdrometer type, corresponding to each mast. With the configuration described, the GLMM is set up as a random-effects Analysis of Variance, and can be expressed as:

$$\begin{aligned}
 y_i &\sim \text{Gamma}(\theta_i, \nu) \\
 \theta_i &= \nu / \mu_i \\
 g(\mu_i) &= \mu + \beta_{t(i)} + \alpha_{m(i)} \\
 \beta_{t(j)} &\sim N(0, \sigma_\beta^2) \\
 \alpha_{m(i)} &\sim N(0, \sigma_\alpha^2)
 \end{aligned} \tag{2}$$

where y_i is the i th observation; ν is a shape parameter; θ_i is a scale parameter that can be expressed in terms of the shape and a mean value corresponding to the i th observation μ_i ; μ is a global mean; $\beta_{t(i)}$ is a parameter accounting for the effect of the disdrometer type corresponding to observation i , $t(i)$; and $\alpha_{m(i)}$ is a parameter accounting for the location (mast) corresponding to observation i , $m(i)$. In our case, we counted with four disdrometers grouped into $t(i) = (1, 2)$ disdrometer types (PARSIVEL and Thies), and located in $m(j) = (1, 2)$ masts, and we set $\beta_1 = \alpha_1 = 0$. For the link function $g(\mu_i)$ we used an identity link, $g(\mu_i) = \mu_i$, except for independent variables r , z , e and NP for which a log link, $g(\mu_i) = \log \mu_i$, was used.

The model in eq. (2) was fitted by generalized least squares (GLS), using the function `lme` from the R library `lme4` (Pinheiro and Bates, 2011). Results from these models allow comparing the means between disdrometer types, while controlling for possible random differences due to the distance between the devices.



3 Results

A total of 58,761 one-minute observations were selected according to the above criteria, from 221 rainfall episodes. Missing values were found in all disdrometers and can be attributed to technical issues (power supply failures, data communication problems, or spurious measures), being Ott PARSIVEL² disdrometers the ones with the highest number of missing values.

5 Thies disdrometers recorded rainfall from 0.001 mm h⁻¹, whereas for PARSIVEL disdrometers the lowest value was 0.007 mm h⁻¹. Therefore, Thies disdrometers recorded more minutes of precipitation, sensing it earlier and longer in comparison with PARSIVEL² disdrometers. Many of these recordings could be catalogued as 'false alarms', but in any case, they suggest a highest sensitivity of Thies disdrometers. To avoid an over-representation of Thies data only the common minutes were analysed, defined as those having records of precipitation rates higher than 0.1 mm h⁻¹ and more than 10 particles in every

10 of the four disdrometers. Table 3 summarizes the data recorded by each disdrometer and selected for the comparison. All types of precipitation events occurring in the sampling site were represented, with the majority of rain minutes corresponding with autumn rains. Rain rates varied between 0.1 mm h⁻¹ and 277 mm h⁻¹. The highest precipitation rates depended on the disdrometer type, being Thies the ones recording the highest rain rates.

[TABLE 3]

15 When considering only the records for which data of the four disdrometers existed, total accumulated precipitation was 397.4 mm (T1), 421 mm (T2), 324.1 mm (P1), and 265.4 mm (P2), where T and P stand for Thies and PARSIVEL², respectively, and 1 and 2 correspond with Mast 1 and Mast 2. Large discrepancies in the cumulative precipitation were therefore found between the devices, which were especially noticeable for the Thies disdrometer located on Mast 2 (T2), which recorded significantly more rainfall (Figure 2). Nevertheless, differences in accumulated Kinetic energy between disdrometer types were smaller than

20 random differences found between masts. As expected, filtered data showed more similarities between disdrometers, since the maximum rain rate was 207.4 mm h⁻¹ (T1), 222.6 mm h⁻¹ (T2), 157.3 mm h⁻¹ (P1), and 181.5 mm h⁻¹ (P2); and total precipitation was 387.5 mm (T1), 406.9 mm (T2), 318.1 mm (P1), and 262.3 mm (P2).

3.1 Example events

Two events were selected to illustrate the differences by disdrometer type. The chosen events are examples of low and high intensity events. Time series of some bulk variables (Figure 3) are compared. In both events, Thies consistently reported a larger number of drops per minute, and also higher rainfall intensities. These differences were most evident in the high intensity event. The rate of kinetic energy ($Ke, J m^{-2}$) did not show as many differences, indicating differences in PSVD recorded by each disdrometer type.



The PSVD plots (Figure 4), depicting the number of drops detected for each combination of drop size and velocity classes during the event by each disdrometer, help explain the differences found. Thus, Thies disdrometers were characterized by a much wider distribution of the PSVD spectra than PARSIVEL² ones. A line showing the theoretical terminal velocity of raindrops as a function of their size (Uplinger, 1981) is also shown as a reference. Although a large majority of drops were found to lie in a region close to the theoretical line, Thies devices showed a larger dispersion around the model and also tended to report a large number of very small particles falling at much higher velocities than those predicted by the theory. These particles, as well as relatively large ones with low falling velocities, seem to be filtered out from the PARSIVEL² output. Finally, there seemed to be a slight underestimation of drop velocity with respect to the theoretical line in PARSIVEL² devices, most notably in the high intensity event and for particles between 1 up to ~ 3 mm. A formal analysis of these differences, considering the whole data set, is presented in the following section.

3.2 Integrated variables, minute scale

Differences between disdrometer types arise for the integrated variables when the whole dataset was analysed, as shown by the exploratory kernel densities plots (Figure 5) and by the GGLMM coefficients (Table 4). Thies disdrometers recorded a much higher number of particles NP (a mean difference of 422 vs. 219), which in turn had an effect on the rainfall intensity R , radar reflectivity Z and kinetic energy E and Ke , which also showed significant differences between disdrometer types. Interestingly, while Z and R were higher on average on Thies, E was lower. Also, the magnitude of the difference was much smaller for R , Z , Ke and E than it could be expected from the strong effect on NP . In comparison to the fixed effects (differences between sensor types), the random effects (effect of the location, or Mast) had an almost negligible size.

[FIGURE 2 and TABLE 4]

Differences in PSVD percentiles were also noticeable and statistically significant. Thus, the higher number of detected particles by Thies disdrometers corresponded to a higher number of smaller and slower drops, as shown by the model coefficients for the variables $D10$, $D50$, $D90$ and $V10$, $V50$, $V90$. The magnitude of the difference was much lower for the highest percentiles ($D90$ and $V90$), albeit significant.

This allows for a better understanding of the differences in the integrated variables between both devices, since the size and velocity distributions have contrasting effects on R , Z , Ke , and E . A higher number of drops detected implies increased values of R and also Z and Ke , although the different distribution of drop sizes helps explain why the larger number of drops detected by Thies did not result in very large differences in these integrated variables, since the average particle size was lower for Thies which reduces the magnitude of the effect. Also, since E depends strongly on the drop size and velocity, and because it is expressed in units of energy per unit rainfall, the smaller particle sizes recorded by Thies resulted in reduced E .



3.3 Integrated variables, event scale

When considering event totals, a similar pattern was found (Figure 6, Table 5). Good agreement by disdrometer type was shown in integrated variables such rain rate (Rm), and reflectivity (Zm) by event. Disdrometer records, by type, slightly differ in maximum rain rate, kinetic energy and mean number of particles by event, with the greatest differences found in PSVD 5 percentiles.

[FIGURE 3 and Table 5]

3.4 Effect of data filtering

When filtered data was used the differences between the two devices were reduced (Table 6 and Appendix Figure 5). Thus, the mean number of particles NP was 280 and 220 for Thies and PARSIVEL, respectively. While the differences in R , Ke and 10 Z did not change much with respect to the previous results, E was now much similar between the two devices. Differences in the PSVD percentiles also got reduced, although they remained significant. At the event scale, when filtered data was used, differences were reduced whereas the pattern remained.

3.5 Effect of rainfall intensity

Data were divided by intensity ranges in order to test if the effect of the disdrometer type changed with different rain intensities. 15 As the rainfall intensity increases, it is expected to find more and bigger drops, which may in turn modify the differences between disdrometer types. Data were thus divided in three intensity groups: low intensity (from 0.1 mm h^{-1} up to 2 mm h^{-1}), medium intensity (from 2 mm h^{-1} up to 10 mm h^{-1}) and high intensity (more than 10 mm h^{-1}). Model coefficients for several integrated variables are given for the three intensity ranges in Table 4, and kernel density plots are given in the Appendix (Figures A.5, A.6, A.7).

20 The differences between disdrometer types were similar at different rainfall intensities, and had the previously mentioned effects, but the magnitude of those effects varied notably. Thus, the differences between disdrometer types were reduced for all variables at the lowest intensity range, while they were maximum for the highest intensity range. During minutes with rainfall intensity higher than 10 mm h^{-1} , for instance, NP was almost nine times higher for Thies than for PARSIVEL. The differences in the PSVD percentiles were also magnified at the highest intensities. Although differences between disdrometer 25 types were reduced when filtered data were compared, the above mentioned tendency remains, becoming especially evident for high intensity rain. In brief, PARSIVEL² tended to underestimate the number of particles recorded, and tended to record a larger number of bigger particles than Thies. At the same time, Thies recorded a very large number of small particles that may mask the amount of bigger particles recorded.



4 Discussion and conclusions

Optical disdrometers are widely used by national weather services as reliable present weather sensors requiring low maintenance. Besides their use as present weather sensors, optical disdrometers provide information on precipitation drop spectra relevant to different research fields and needed for precipitation intercomparison and radar calibration experiments. Precipitation remote sensing and precipitation estimation together with soil erosion are most interested in accurate measurements of raindrop size and velocity, since environmental processes are influenced not only by precipitation amount and intensity but also how it is structured in individual drops. Studies on this topic are present in scientific literature, first evaluating impact disdrometers and then optical disdrometers (Kinnell, 1976; Rosewell, 1986; Tokay et al., 2001; Krajewski et al., 2006; Lanza and Vuerich, 2009; Thurai et al., 2011). Reliable measurements of precipitation particle spectra have to take into account the influence of sensor type and accuracy in relation with precipitation regimes, since such measurement uncertainty is contained in the final precipitation estimation and subsequent models results (Angulo-Martínez and Barros, 2015). Current optical disdrometers are good commercially affordable tools able to provide a complete description of precipitation.

The accuracy of optical disdrometers may be affected by a number of factors, such as wind and turbulence conditions, which may modify particles vertical trajectory and therefore, measurements (Nespor et al., 2000; Habib and Krajewski, 2001). The measurement principle is based in laser beam power decrease with beam obscuration, and current interruption, when particles pass through the laser area. Frasson et al. (2011) evaluated the performance of Thies optical disdrometer and found that it underestimated particles diameter by ~ 0.5 mm, indicating as possible reason the non-homogeneous beam power distribution. When power supply for the laser is homogeneous there is a linear relation between the particle shaded area and the amount of energy that reached the receiver photodiode, being this the principle that allows particle size measurement. However, oscillations in the current may drift the estimations. In addition, depending on where on the laser sampling area the particle pass, mis-detection could be greater. For instance, particles passing through the laser closer to the heads of PARSIVEL disdrometer were less sensed than those that passed in the center (Frasson et al., 2011; Angulo-Martínez and Barros, 2015). Measurement inaccuracy is also related to their inability to correctly identify simultaneous drops, which are sensed as single drops much larger in size. Raasch and Umhauer (1984) investigated with computer simulations the ability of optical disdrometers for detecting simultaneous drops, founding a probability of 10% during intense events, so this effect must not be disregarded. They provided an algorithm to fix the problem in their prototype internal software (Raasch and Umhauer, 1984). Another measurement problem is related with margining fallers, i.e. drops that partially fall in the sampling area (Yuter et al., 2006) and are sensed with a smaller size than they really are, but with their complete velocity. A correction for this effect has been proposed based on modifying the effective sampling area depending on the particle size (Löffler-Mang and Joss, 2000; Battaglia et al., 2010; Raupach and Berne, 2015). Hauser et al. (1984) detected an unsuppressed 50Hz rumble noise in the power supply which interfered with the measurement of particles smaller than 0.3 mm. Therefore, common agreement stated from the literature is the baseline of 0.3 mm of diameter as starting point for measuring particle sizes. This threshold has been built in the Joss and Waldvogel impact disdrometer (Joss and Waldvogel, 1967) and in 2DVD (Kruger and Krajewski, 2002). PARSIVEL disdrometer (all of



its versions) leave empty the two initial diameter bins in order to avoid the the low signal-to-noise ratio, as JWD and 2DVD, whereas Thies disdrometer does not, starting drop size measures from 0.187 mm. Thies high sensitivity has been previously pointed out indicating that 0.001 mm h^{-1} rain rate were not sensed by other meteorological devices or observer, declaring the measure as "false alarm" (Upton and Brawn, 2008).

5 Disdrometer external structure may intercept precipitation particles, which eventually break and splash away in smaller but accelerated drops. PARSIVEL disdrometers include a splashing shield in their design to reduce such effect, while Thies disdrometers do not. Splashed particles are known in the literature (Kathiravelu et al., 2016). They could be removed by abnormal size-fall velocity pairs.

All these effects increase with precipitation intensity, triggering unreal intensity peaks with high variability among sensors and by sensor type as a consequence of measurement inaccuracies and environmental influences (Donnadieu et al., 1969; Lazinger et al., 2006; Lanza and Vuerich, 2009; Frasson et al., 2011). The results shown in this study agree with previous works regarding precipitation spectra measurements during high intensity rains. The two types of disdrometer analysed showed different PSD populations for the same rainfall events. When PSVD data were filtered, considering only particles with diameters greater than 0.3 mm, these differences were reduced, although the tendency remains and increases for high intensity rains. 15 Frasson et al. (2011) and ? also noted the same result. Articles in scientific literature comparing Ott PARSIVEL² disdrometer measurements with more accurate ones such as 2DVD (Raupach and Berne, 2015) and as JDW (Tokay et al., 2014) indicated that PARSIVEL² overestimated the number of drops smaller than 1 mm and larger than 3.25 mm while underestimating the number of drops between 1.38 mm - 3.25 mm. Very good agreement was found for diameter size estimation between PARSIVEL² and JWD between 0.7 mm - 3 mm, while large drops ($\phi > 3 \text{ mm}$) may be overestimated by PARSIVEL² (Tokay 20 et al., 2014; Park et al., 2017). The study of Tokay et al. (2014) highlighted a better detection of rain/no rain by PARSIVEL² in comparison with the previous PARSIVEL versions. This was also noted by Angulo-Martínez and Barros (2015). However, when comparing PARSIVEL² with Thies, the last one was more sensitive to precipitation detection, previously noted by cite-upton2008 and shown by our results. Regarding fall velocity measurements, Thies provided a better estimation in comparison with theoretical terminal velocity, whereas PARSIVEL² tended to underestimate fall velocity especially for midsize drops (1 25 mm - 3 mm). PARSIVEL manufacture recognised a problem in velocity underestimation, which is in fixing process (Tokay et al., 2014).

In the present study there are no differences regarding the influence of the hydrometeorological regimes, nevertheless collocated optical disdrometers showed differences in precipitation spectra measurements increasing with rain rate. Such differences should be taken into account in relation with the hydrometeorological regime. For instance, in regions prone to small rain- 30 drop spectra PARSIVEL² disdrometer may underestimate precipitation measurements, since its best performance is achieved between 1 mm - 3 mm particles size (Jaffrain and Berne, 2011; Angulo-Martínez, 2015). However, in areas with midsize precipitation hydrometeorological regimes PARSIVEL² will perform better.



Sumarizing, Thies devices recorded a much larger number of drops than PARSIVEL², but also a much larger spread of the PSVD spectra, with a significant amount of drops with unusual combinations of size and velocity. Most notably, a large number of small drops with excessively high velocities were consistently reported by Thies disdrometers. PARSIVEL² devices, on the contrary, recorded less drops but PSVD spectra much closer to the theoretical model, with a tendency towards underestimating drop velocity. This resulted in significant discrepancies between both disdrometer types in all bulk precipitation parameters such as rain intensity and amount, radar reflectivity, or kinetic energy. These differences may be explained by hardware or software differences. More stable and homogeneous laser beams translate directly to a better estimation of drop size and velocity. The external design may also have a large influence on the drop splash. In the technical description of the PARSIVEL² disdrometer it is mentioned that its design incorporates protections against double drop and partial drop detections or margin fallers, although the exact procedures are not documented. The inspection of the resulting PVSD spectra plots suggests that these corrections are achieved by post-processing the raw data matrix, i.e. by filtering-out the anomalous drops with respect to a theoretical model. This would be of course an advantage for the average user, but prevents the advanced user from developing and using custom-made solutions.

Code availability. (Beguería et al., 2017)

15 *Competing interests.* We declare that we have no competing interests

Acknowledgements. This work has been supported by the research project CGL2014-52135-C3-1-R, financed by the Spanish Ministerio de Economía, Industria y Competitividad (MINECO) and EU-FEDER. The work of M. Angulo-Martínez was supported by a postdoctoral grant by MINECO.



References

- Adirosi, E. b., Baldini, L., Roberto, N., Gatlin, P., and Tokay, A. e.: Improvement of vertical profiles of raindrop size distribution from micro rain radar using 2D video disdrometer measurements, *Atmospheric Research*, 169, 404–415, <https://doi.org/10.1016/j.atmosres.2015.07.002>, 2016.
- 5 Angulo-Martínez, M. and Barros, A.: Measurement uncertainty in rainfall kinetic energy and intensity relationships for soil erosion studies: An evaluation using PARSIVEL disdrometers in the Southern Appalachian Mountains, *Geomorphology*, 228, 28–40, <https://doi.org/10.1016/j.geomorph.2014.07.036>, 2015.
- Angulo-Martínez, M., Beguería, S., Navas, A., and Machín, J.: Splash erosion under natural rainfall on three soil types in NE Spain, *Geomorphology*, 175–176, 38–44, <https://doi.org/10.1016/j.geomorph.2012.06.016>, 2012.
- 10 Angulo-Martínez, M., Beguería, S., and Kysely, J.: Use of disdrometer data to evaluate the relationship of rainfall kinetic energy and intensity (KE-I), *Science of the Total Environment*, 568, 83–94, <https://doi.org/10.1016/j.scitotenv.2016.05.223>, 2016.
- Atlas, D. b. f., Ulbrich, C. g., Marks Jr., F. h., Amitai, E. i., and Williams, C. j.: Systematic variation of drop size and radar-rainfall relations, *Journal of Geophysical Research Atmospheres*, 104, 6155–6169, 1999.
- Battaglia, A., Rustemeier, E., Tokay, A. c., Blahak, U., and Simmer, C.: PARSIVEL snow observations: A critical assessment, *Journal of Atmospheric and Oceanic Technology*, 27, 333–344, <https://doi.org/10.1175/2009JTECHA1332.1>, 2010.
- 15 Beguería, S., Latorre, B., and Angulo-Martínez, M.: DisdRo: an R package for working with disdrometric data, <https://github.com/sbegueria/disdRo>, 2017.
- Brawn, D. and Upton, G.: On the measurement of atmospheric gamma drop-size distributions, *Atmospheric Science Letters*, 9, 245–247, <https://doi.org/10.1002/asl.198>, 2008.
- 20 Calheiros, A. and Machado, L.: Cloud and rain liquid water statistics in the CHUVA campaign, *Atmospheric Research*, 144, 126–140, <https://doi.org/10.1016/j.atmosres.2014.03.006>, 2014.
- Castro, A., Alonso-Blanco, E., González-Colino, M., Calvo, A., Fernández-Raga, M., and Fraile, R.: Aerosol size distribution in precipitation events in León, Spain, *Atmospheric Research*, 96, 421–435, <https://doi.org/10.1016/j.atmosres.2010.01.014>, 2010.
- Ciaccioni, A., Bezak, N., and Rusjan, S.: Analysis of rainfall erosivity using disdrometer data at two stations in central Slovenia, *Acta hydrotechnica*, 29, 89–101, 2016.
- 25 Cruse, R., Flanagan, D., Frankenberger, J., Gelder, B., Herzmann, D., James, D., Krajewski, W., Kraszewski, M., Lafflen, J., Opsomer, J., and Today, D.: Daily estimates of rainfall, water runoff, and soil erosion in Iowa, *Journal of Soil and Water Conservation*, 61, 191–199, 2006.
- Donnadieu, G., Dubosclard, G., and Godard, S.: Un pluviometre ophotoelctrique pour la determination simultanee des spectres dimensionnel at de vitesse de chute des gouttes de pluie, *J. Res. Atmos.*, 4, 1969.
- 30 Fernández-Raga, M., Fraile, R., Keizer, J., Varela Teijeiro, M., Castro, A., Palencia, C., Calvo, A., Koenders, J., and Da Costa Marques, R.: The kinetic energy of rain measured with an optical disdrometer: An application to splash erosion, *Atmospheric Research*, 96, 225–240, <https://doi.org/10.1016/j.atmosres.2009.07.013>, 2010.
- Frasson, R., da Cunha, L., and Krajewski, W.: Assessment of the Thies optical disdrometer performance, *Atmospheric Research*, 101, 237–255, <https://doi.org/10.1016/j.atmosres.2011.02.014>, 2011.
- 35 Gires, A., Tchiguirinskaia, I., and Schertzer, D.: Multifractal comparison of the outputs of two optical disdrometers, *Hydrological Sciences Journal*, pp. 1–11, <https://doi.org/10.1080/02626667.2015.1055270>, 2016.



- Hauser, D., Amayenc, P., Nutten, B., and Waldteufel, P.: A New Optical Instrument for Simultaneous Measurement of Raindrop Diameter and Fall Speed Distributions, *J. Atmos. Oceanic Technol.*, 1, 256–269, [https://doi.org/10.1175/1520-0426\(1984\)001<0256:ANOIFS>2.0.CO;2](https://doi.org/10.1175/1520-0426(1984)001<0256:ANOIFS>2.0.CO;2), 1984.
- Iguchi, T., Kozu, T., Meneghini, R., Awaka, J., and Okamoto, K.: Rain-profiling algorithm for the TRMM precipitation radar, *Journal of Applied Meteorology*, 39, 2038–2052, 2000.
- Ioannidou, M., Kalogiros, J., and Stavrakis, A.: Comparison of the TRMM Precipitation Radar rainfall estimation with ground-based disdrometer and radar measurements in South Greece, *Atmospheric Research*, 181, 172–185, <https://doi.org/10.1016/j.atmosres.2016.06.023>, 2016.
- Iserloh, T., Ries, J., Arnáez, J., Boix-Fayos, C., Butzen, V., Cerdà, A., Echeverría, M., Fernández-Gálvez, J., Fister, W., Geißler, C., Gómez, J., Gómez-Macpherson, H., Kuhn, N., Lázaro, R., León, F., Martínez-Mena, M., Martínez-Murillo, J., Marzen, M., Mingorance, M., Ortigosa, L., Peters, P., Regüés, D., Ruiz-Sinoga, J., Scholten, T., Seeger, M. I., Solé-Benet, A., Wengel, R., and Wirtz, S.: European small portable rainfall simulators: A comparison of rainfall characteristics, *Catena*, 110, 100–112, <https://doi.org/10.1016/j.catena.2013.05.013>, 2013.
- Jaffrain, J. and Berne, A.: Experimental quantification of the sampling uncertainty associated with measurements from PARSIVEL disdrometers, *Journal of Hydrometeorology*, 12, 352–370, <https://doi.org/10.1175/2010JHM1244.1>, 2011.
- Jaffrain, J. and Berne, A.: Quantification of the small-scale spatial structure of the raindrop size distribution from a network of disdrometers, *Journal of Applied Meteorology and Climatology*, 51, 941–953, <https://doi.org/10.1175/JAMC-D-11-0136.1>, 2012.
- Jameson, A., Larsen, M., and Kostinski, A.: Disdrometer network observations of finescale spatial-temporal clustering in rain, *Journal of the Atmospheric Sciences*, 72, 1648–1666, <https://doi.org/10.1175/JAS-D-14-0136.1>, 2015.
- Jameson, A. c. and Kostinski, A.: Fluctuation properties of precipitation. Part II: Reconsideration of the meaning and measurement of raindrop size distributions, *Journal of the Atmospheric Sciences*, 55, 283–294, 1998.
- Jayawardena, A. b. and Rezaur, R.: Drop size distribution and kinetic energy load of rainstorms in Hong Kong, *Hydrological Processes*, 14, 1069–1082, [https://doi.org/10.1002/\(SICI\)1099-1085\(20000430\)14:6<1069::AID-HYP997>3.0.CO;2-Q](https://doi.org/10.1002/(SICI)1099-1085(20000430)14:6<1069::AID-HYP997>3.0.CO;2-Q), 2000.
- Joss, J. and Waldvogel, A.: Ein Spektrograph für Niederschlagstropfen mit automatischer Auswertung, *PAGEOPH*, 68, 240–246, <https://doi.org/10.1007/BF00874898>, 1967.
- Kathiravelu, G., Lucke, T., and Nichols, P.: Rain drop measurement techniques: A review, *Water (Switzerland)*, 8, <https://doi.org/10.3390/w8010029>, 2016.
- Kinnell, P. I. A.: Some Observations on the Joss-Waldvogel Rainfall Disdrometer, *J. Appl. Meteor.*, 15, 499–502, [https://doi.org/10.1175/1520-0450\(1976\)015<0499:SOOTJW>2.0.CO;2](https://doi.org/10.1175/1520-0450(1976)015<0499:SOOTJW>2.0.CO;2), 1976.
- Krajewski, W., Kruger, A., and Nespor, V.: Experimental and numerical studies of small-scale rainfall measurements and variability, *Water Science and Technology*, 37, 131–138, [https://doi.org/10.1016/S0273-1223\(98\)00325-4](https://doi.org/10.1016/S0273-1223(98)00325-4), conference of Proceedings of the 1997 3rd International Workshop on Rainfall in Urban Areas ;, 1998.
- Krajewski, W., Kruger, A., Caracciolo, C., Golé, P., Barthes, L., Creutin, J.-D., Delahaye, J.-Y., Nikolopoulos, E., Ogden, F., and Vinson, J.-P.: DEVEX-disdrometer evaluation experiment: Basic results and implications for hydrologic studies, *Advances in Water Resources*, 29, 311–325, <https://doi.org/10.1016/j.advwatres.2005.03.018>, 2006.
- Kruger, A. and Krajewski, W.: Two-dimensional video disdrometer: A description, *Journal of Atmospheric and Oceanic Technology*, 19, 602–617, 2002.



- Lanza, L. and Vuerich, E.: The WMO Field Intercomparison of Rain Intensity Gauges, *Atmospheric Research*, 94, 534–543, <https://doi.org/10.1016/j.atmosres.2009.06.012>, 2009.
- Lazinger, E., Theel, M., and Windoph, H.: Rainfall amount and intensity measured by the Thies laser precipitation monitor, in: WMO Technical Conference on Instruments and Methods of Observation (TECO-2006), Geneva, Switzerland, 2006.
- 5 Löffler-Mang, M. and Blahak, U.: Estimation of the equivalent radar reflectivity factor from measured snow size spectra, *Journal of Applied Meteorology*, 40, 843–849, 2001.
- Löffler-Mang, M. and Joss, J.: An optical disdrometer for measuring size and velocity of hydrometeors, *Journal of Atmospheric and Oceanic Technology*, 17, 130–139, 2000.
- Liao, L., Meneghini, R., and Tokay, A.: Uncertainties of GPM DPR rain estimates caused by DSD parameterizations, *Journal of Applied Meteorology and Climatology*, 53, 2524–2537, <https://doi.org/10.1175/JAMC-D-14-0003.1>, 2014.
- 10 Loik, M., Breshears, D., Lauenroth, W., and Belnap, J.: A multi-scale perspective of water pulses in dryland ecosystems: Climatology and ecohydrology of the western USA, *Oecologia*, 141, 269–281, <https://doi.org/10.1007/s00442-004-1570-y>, 2004.
- Marzano, F. d., Cimini, D. d. d., and Montopoli, M. d. d.: Investigating precipitation microphysics using ground-based microwave remote sensors and disdrometer data, *Atmospheric Research*, 97, 583–600, <https://doi.org/10.1016/j.atmosres.2010.03.019>, 2010.
- 15 Miriovsky, B., Bradley, A., Eichinger, W., Krajewski, W., Kruger, A., Nelson, B., Creutin, J.-D., Lapetite, J.-M., Lee, G., Zawadzki, I., and Ogden, F.: An experimental study of small-scale variability of radar reflectivity using disdrometer observations, *Journal of Applied Meteorology*, 43, 106–118, 2004.
- Olsen, R., Rogers, D., and Hodge, D.: The aRb Relation in the Calculation of Rain Attenuation, *IEEE Transactions on Antennas and Propagation*, 26, 318–329, <https://doi.org/10.1109/TAP.1978.1141845>, 1978.
- 20 Park, S.-G., Kim, H.-L., Ham, Y.-W., and Jung, S.-H.: Comparative evaluation of the OTT PARSIVEL2 using a collocated two-dimensional video disdrometer, *Journal of Atmospheric and Oceanic Technology*, 34, 2059–2082, <https://doi.org/10.1175/JTECH-D-16-0256.1>, 2017.
- Petan, S., Rusjan, S., Vidmar, A., and Mikoš, M.: The rainfall kinetic energy-intensity relationship for rainfall erosivity estimation in the mediterranean part of Slovenia, *Journal of Hydrology*, 391, 314–321, <https://doi.org/10.1016/j.jhydrol.2010.07.031>, 2010.
- Pinheiro, J. G. and Bates, D.: *Mixed-Effects Models in S and S-PLUS*, Springer, New York, NY, 2000.
- 25 Raasch, J. and Umhauer, H.: Errors in the Determination of Particle Size Distributions Caused by coincidences in optical particle counters, *Particle & Particle Systems Characterization*, 1, 53–58, <https://doi.org/10.1002/ppsc.19840010109>, 1984.
- Raupach, T. and Berne, A.: Correction of raindrop size distributions measured by Parsivel disdrometers, using a two-dimensional video disdrometer as a reference, *Atmospheric Measurement Techniques*, 8, 343–365, <https://doi.org/10.5194/amt-8-343-2015>, 2015.
- Raupach, T. and Berne, A.: Small-scale variability of the raindrop size distribution and its effect on areal rainfall retrieval, *Journal of Hydrometeorology*, 17, 2077–2104, <https://doi.org/10.1175/JHM-D-15-0214.1>, 2016.
- 30 Rosewell, C.: Rainfall kinetic energy in eastern Australia., *Journal of Climate & Applied Meteorology*, 25, 1695–1701, 1986.
- Salles, C., Sempere-Torres, D., and Creutin, J.-D.: Characterisation of raindrop size distribution in Mediterranean climate: analysis of the variations on the Z-R relationship, in: *Conference on Radar Meteorology*, pp. 670–673, American Meteorological Soc, Boston, MA, United States, Montreal, Que., Can, 1999.
- 35 Sanchez-Moreno, J., Mannaerts, C., Jetten, V., and Löffler-Mang, M.: Rainfall kinetic energy-intensity and rainfall momentum-intensity relationships for Cape Verde, *Journal of Hydrology*, 454-455, 131–140, <https://doi.org/10.1016/j.jhydrol.2012.06.007>, 2012.
- Sempere-Torres, D., Porrà, J., and Creutin, J.-D.: Experimental evidence of a general description for raindrop size distribution properties, *Journal of Geophysical Research Atmospheres*, 103, 1785–1797, 1998.



- Sheppard, B. and Joe, P.: Comparison of raindrop size distribution measurements by a Joss- Waldvogel disdrometer, a PMS 2DG spectrometer, and a POSS Doppler radar, *Journal of Atmospheric & Oceanic Technology*, 11, 874–887, 1994.
- Shuttleworth, W.: *Terrestrial Hydrometeorology*, Wiley-Blackwell, 2012.
- Tan, J., Petersen, W., and Tokay, A.: A novel approach to identify sources of errors in IMERG for GPM ground validation, *Journal of Hydrometeorology*, 17, 2477–2491, <https://doi.org/10.1175/JHM-D-16-0079.1>, 2016.
- 5 Tapiador, F., Checa, R., and De Castro, M.: An experiment to measure the spatial variability of rain drop size distribution using sixteen laser disdrometers, *Geophysical Research Letters*, 37, <https://doi.org/10.1029/2010GL044120>, 2010.
- Tapiador, F., Navarro, A., Moreno, R., Jiménez-Alcázar, A., Marcos, C., Tokay, A., Durán, L., Bodoque, J., Martín, R., Petersen, W., and de Castro, M.: On the optimal measuring area for pointwise rainfall estimation: A dedicated experiment with 14 laser disdrometers, *Journal of Hydrometeorology*, 18, 753–760, <https://doi.org/10.1175/JHM-D-16-0127.1>, 2017.
- 10 Testud, J., Oury, S., Black, R., Amayenc, P., and Dou, X.: The concept of "normalized" distribution to describe raindrop spectra: A tool for cloud physics and cloud remote sensing, *Journal of Applied Meteorology*, 40, 1118–1140, 2001.
- Thurai, M. and Bringi, V.: *Rain microstructure from polarimetric radar and advanced disdrometers*, Springer Berlin Heidelberg, 2008.
- Thurai, M., Petersen, W., Tokay, A., Schultz, C., and Gatlin, P.: Drop size distribution comparisons between Parsivel and 2-D video disdrometers, *Advances in Geosciences*, 30, 3–9, <https://doi.org/10.5194/adgeo-30-3-2011>, 2011.
- 15 Tokay, A., Kruger, A., and Krajewski, W.: Comparison of drop size distribution measurements by impact and optical disdrometers, *Journal of Applied Meteorology*, 40, 2083–2097, 2001.
- Tokay, A., Petersen, W. A., Gatlin, P., and Wingo, M.: Comparison of Raindrop Size Distribution Measurements by Collocated Disdrometers, *Journal of Atmospheric and Oceanic Technology*, 30, 1672–1690, <https://doi.org/10.1175/JTECH-D-12-00163.1>, 2013.
- 20 Tokay, A. b., Wolff, D., and Petersen, W.: Evaluation of the new version of the laser-optical disdrometer, OTT parsivel, *Journal of Atmospheric and Oceanic Technology*, 31, 1276–1288, <https://doi.org/10.1175/JTECH-D-13-00174.1>, 2014.
- Uijlenhoet, R. and Sempere, T.: Measurement and parameterization of rainfall microstructure, *Journal of Hydrology*, 328, 1–7, <https://doi.org/10.1016/j.jhydrol.2005.11.038>, 2006.
- Ulbrich, C.: Natural variations in the analytical form of the raindrop size distribution., *Journal of Climate & Applied Meteorology*, 22, 1764–1775, 1983.
- 25 Upton, G. and Brawn, D.: An investigation of factors affecting the accuracy of Thies disdrometers, in: *WMO Technical Conference on Instruments and Methods of Observation (TECO-2008)*, St. Petersburg, Russian Federation, pp. 27–29, 2008.
- Yuter, S., Kingsmill, D., Nance, L., and Löffler-Mang, M.: Observations of precipitation size and fall speed characteristics within coexisting rain and wet snow, *Journal of Applied Meteorology and Climatology*, 45, 1450–1464, 2006.
- 30 Zhang, L., Zhao, L., Xie, C., Liu, G., Gao, L., Xiao, Y., Shi, J., and Qiao, Y.: Intercomparison of solid precipitation derived from the weighting rain gauge and optical instruments in the interior Qinghai-Tibetan plateau, *Advances in Meteorology*, 2015, <https://doi.org/10.1155/2015/936724>, 2015.



[TABLES AND FIGURES]

Table 1. Mean particle size and velocity bins by disdrometer type

Mean particle diameter bins		Mean particle velocity bins	
Thies	PARSIVEL	Thies	PARSIVEL
0.187	0.062	0.1	0.05
0.313	0.187	0.3	0.15
0.437	0.312	0.5	0.25
0.625	0.437	0.7	0.35
0.875	0.562	0.9	0.45
1.125	0.687	1.2	0.55
1.375	0.812	1.6	0.65
1.625	0.937	2	0.75
1.875	1.062	2.4	0.85
2.25	1.187	2.8	0.95
2.75	1.375	3.2	1.1
3.25	1.625	3.8	1.3
3.75	1.875	4.6	1.5
4.25	2.125	5.4	1.7
4.75	2.375	6.2	1.9
5.25	2.75	7	2.2
6.25	3.25	7.8	2.6
6.75	3.75	8.6	3
7.25	4.25	9.5	3.4
7.75	4.75	10.5	3.8
8.25	5.5		4.4
9	6.5		5.2
	7.5		6
	8.5		6.8
	9.5		7.6
	11		8.8
	13		10.4
	15		12
	17		13.6
	19		15.2
	21.5		17.6
	24.5		20.8



Table 2. Disdrometer evaluated variables. *M* and *m* stand for max and mean, respectively.

Variables	Units	Acronym
Rain rate, mean and max	mm h ⁻¹	<i>R, Rm, RM</i>
Precipitation accumulated	mm	<i>P</i>
Reflectivity	dB mm ⁶ m ⁻³	<i>Z</i>
Kinetic energy rate	J m ⁻²	<i>Ke, Kem, KeM</i>
Unit Kinetic energy	J m ⁻² mm ⁻¹	<i>E, Em, EM</i>
Number of particles	unit	<i>NP, NPM</i>
10th PSD percentile	mm	<i>D10</i>
50th PSD percentile	mm	<i>D50</i>
90th PSD percentile	mm	<i>D90</i>
10th PVD percentile	m s ⁻¹	<i>V10</i>
50th PVD percentile	m s ⁻¹	<i>V50</i>
90th PVD percentile	m s ⁻¹	<i>V90</i>



Table 3. Disdrometer data summary. Percentage of records from every disdrometer corresponding to the categories. Total one-min records with $I > 0.1 \text{ mm h}^{-1}$ and $NP > 10$ are: 58761. Recorded by at least two disdrometers of different type.

Variables	M1-Thies	M2-Thies	M1-PARSIVEL	M2-PARSIVEL
N records (%)	26.7	26.6	26.8	20
Nr winter	27.7	27.7	28.7	33.7
Nr spring	26.6	26.1	25.3	10.9
Nr summer	11.1	11.1	11.1	11.9
Nr autumn	34.6	35.2	35.0	43.5
Nr $0.1\text{-}2 \text{ mm h}^{-1}$	84.6	83.6	86.8	85.8
Nr $2\text{-}5 \text{ mm h}^{-1}$	11.9	12.4	10.4	11.1
Nr $5\text{-}10 \text{ mm h}^{-1}$	2.3	2.8	1.9	2.0
Nr $10\text{-}25 \text{ mm h}^{-1}$	0.75	0.8	0.7	0.59
Nr $R > 25 \text{ mm h}^{-1}$	0.43	0.46	0.3	0.49
max R (mm h^{-1})	251	277	170	169



Table 4. Gamma Generalized Linear Mixed-Effects Models coefficients for one-minute records. Analysis done with a sample size of $N = 1000$.

Var	All Intensity records					$0.1 < I < 2 \text{ mm h}^{-1}$				
	Thies	Parsi	Res St Err	Mast	p-val	Thies	Parsi	Res St Err	Mast	p-val
<i>R</i>	1.889	1.523	4.210	0.000	<0.001	0.599	0.575	0.726	0.004	<0.001
<i>Z</i>	22.78	22.29	0.333	0.005	<0.001	19.65	19.36	0.276	0.005	<0.001
<i>Ke</i>	0.469	0.459	8.827	0.450	<0.001	0.100	0.096	1.060	0.019	<0.001
<i>E</i>	9.845	10.49	0.532	0.000	<0.001	8.645	8.785	0.457	0.007	<0.001
<i>NP</i>	422.3	219.2	2.488	0.000	<0.001	205.0	155.7	0.710	0.012	<0.001
<i>D10</i>	0.237	0.475	0.217	0.002	<0.001	0.249	0.468	0.214	0.001	<0.001
<i>D50</i>	0.505	0.759	0.214	0.000	<0.001	0.531	0.733	0.208	0.000	<0.001
<i>D90</i>	1.078	1.220	0.257	0.003	<0.001	1.050	1.130	0.236	0.003	<0.001
<i>V10</i>	1.210	1.860	0.228	0.019	<0.001	1.262	1.814	0.226	0.011	<0.001
<i>V50</i>	2.283	2.955	0.166	0.008	<0.001	2.357	2.876	0.167	0.002	<0.001
<i>V90</i>	4.050	4.101	0.182	0.000	<0.001	3.978	3.911	0.168	0.005	<0.001
Var	$2 < I < 10 \text{ mm h}^{-1}$					$I > 10 \text{ mm h}^{-1}$				
	Thies	Parsi	Res St Err	Mast	Signf	Thies	Parsi	Res St Err	Mast	Signf
<i>R</i>	4.195	3.561	0.386	0.014	<0.001	53.30	32.01	0.902	0.000	<0.001
<i>Z</i>	33.05	32.17	0.099	0.004	<0.001	46.93	45.87	0.117	0.000	<0.001
<i>Ke</i>	1.027	1.012	0.636	0.030	<0.001	18.20	15.37	0.924	0.121	<0.001
<i>E</i>	14.21	16.20	0.334	0.011	<0.001	19.59	28.62	0.297	0.038	<0.001
<i>NP</i>	827.2	441.4	0.452	0.006	<0.001	9056	1186	0.756	0.000	<0.001
<i>D10</i>	0.196	0.506	0.168	0.002	<0.001	0.161	0.506	0.160	0.001	<0.001
<i>D50</i>	0.451	0.862	0.218	0.000	<0.001	0.305	1.006	0.220	0.002	<0.001
<i>D90</i>	1.198	1.505	0.177	0.008	<0.001	0.796	2.257	0.311	0.000	<0.001
<i>V10</i>	1.019	2.048	0.185	0.026	<0.001	0.850	2.044	0.244	0.051	<0.001
<i>V50</i>	2.178	3.273	0.161	0.029	<0.001	1.823	3.578	0.190	0.086	<0.001
<i>V90</i>	4.439	4.458	0.132	0.000	<0.001	4.193	6.575	0.158	0.127	<0.001



Table 5. Gamma Generalized Linear Mixed-Effects Models coefficients for event means. N = 221.

Variable	All Intensity records				
	Thies	Parsi	St Err	Mast	p-val
<i>Rm</i>	1.51	1.18	2.88	0.00	<0.001
<i>RM</i>	7.84	6.56	3.26	0.00	<0.001
<i>Zm</i>	20.4	20.2	0.26	0.00	<0.001
<i>Kem</i>	0.36	0.34	3.53	0.00	<0.001
<i>KeM</i>	3.95	4.86	3.74	0.00	<0.001
<i>Em</i>	10.3	10.8	0.40	0.00	<0.001
<i>EM</i>	19.0	23.0	0.53	0.00	<0.001
<i>Npm</i>	320	147	2.07	0.00	<0.001



Table 6. Filtered data Gamma Generalized Linear Mixed-Effects Models coefficients for one-minute records. Analysis done with a sample size of $N = 1000$.

Var	All Intensity records					$0.1 < I < 2 \text{ mm h}^{-1}$				
	Thies	Parsi	Res St Err	Mast	p-val	Thies	Parsi	Res St Err	Mast	p-val
<i>R</i>	1.820	1.470	3.630	0.000	<0.001	0.605	0.565	0.726	0.004	<0.001
<i>Z</i>	23.71	22.26	0.350	0.005	<0.001	20.35	19.27	0.276	0.003	<0.001
<i>Ke</i>	0.445	0.431	6.509	0.542	<0.001	0.102	0.079	1.060	0.021	<0.001
<i>E</i>	9.760	8.630	0.540	0.011	<0.001	8.72	7.301	0.457	0.007	<0.001
<i>NP</i>	283.2	220.7	1.580	0.010	<0.001	163.0	153.24	0.710	0.016	<0.001
<i>D10</i>	0.345	0.489	0.165	0.003	<0.001	0.353	0.482	0.180	0.002	<0.001
<i>D50</i>	0.613	0.766	0.190	0.003	<0.001	0.620	0.741	0.195	0.003	<0.001
<i>D90</i>	1.172	1.212	0.249	0.003	<0.001	1.116	1.130	0.236	0.002	<0.001
<i>V10</i>	1.336	1.853	0.214	0.017	<0.001	1.395	1.812	0.218	0.012	<0.001
<i>V50</i>	2.441	2.938	0.178	0.022	<0.001	2.472	2.864	0.176	0.015	<0.001
<i>V90</i>	4.173	4.031	0.182	0.000	<0.001	4.074	3.876	0.173	0.007	<0.001
Var	$2 < I < 10 \text{ mm h}^{-1}$					$I > 10 \text{ mm h}^{-1}$				
	Thies	Parsi	Res St Err	Mast	p-val	Thies	Parsi	Res St Err	Mast	p-val
<i>R</i>	4.154	3.536	0.378	0.012	<0.001	49.16	34.23	0.859	0.000	<0.001
<i>Z</i>	35.06	32.59	0.122	0.005	<0.001	52.88	47.42	0.155	0.005	<0.001
<i>Ke</i>	0.989	0.824	0.690	0.035	<0.001	16.95	17.34	0.947	0.000	<0.001
<i>E</i>	13.92	13.36	0.385	0.011	<0.001	19.71	27.94	0.309	0.000	<0.001
<i>NP</i>	558.4	431.0	0.421	0.000	<0.001	3619	1125	0.670	0.000	<0.001
<i>D10</i>	0.317	0.521	0.138	0.000	<0.001	0.290	0.523	0.173	0.000	<0.001
<i>D50</i>	0.601	0.871	0.173	0.000	<0.001	0.446	1.022	0.235	0.002	<0.001
<i>D90</i>	1.394	1.531	0.177	0.008	<0.001	1.293	2.314	0.236	0.020	<0.001
<i>V10</i>	1.145	2.001	0.186	0.010	<0.001	0.791	1.943	0.275	0.000	<0.001
<i>V50</i>	2.349	3.210	0.186	0.021	<0.001	1.504	3.428	0.232	0.000	<0.001
<i>V90</i>	4.618	4.674	0.167	0.004	<0.001	3.755	6.543	0.227	0.033	<0.001



Figure 1. Sampling site with four collocated disdrometers

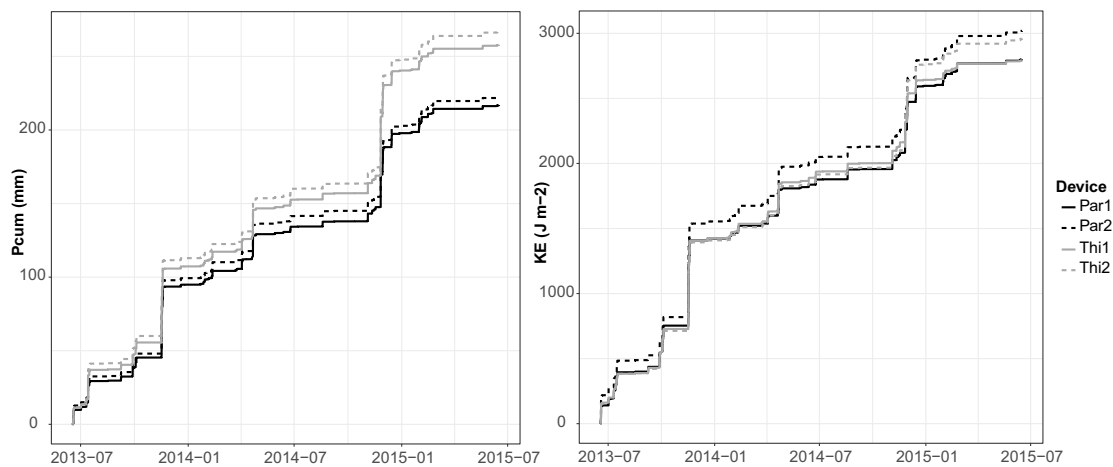
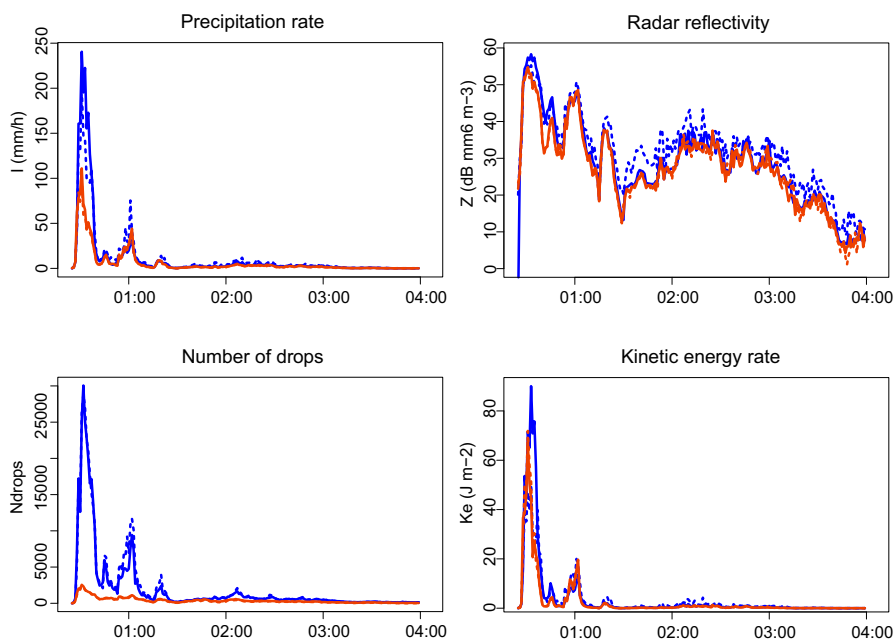


Figure 2. Accumulated precipitation (mm) and Kinetic energy (J m^{-2}) during the two years experiment.



High Intensity Event: E365



Low Intensity Event: E455

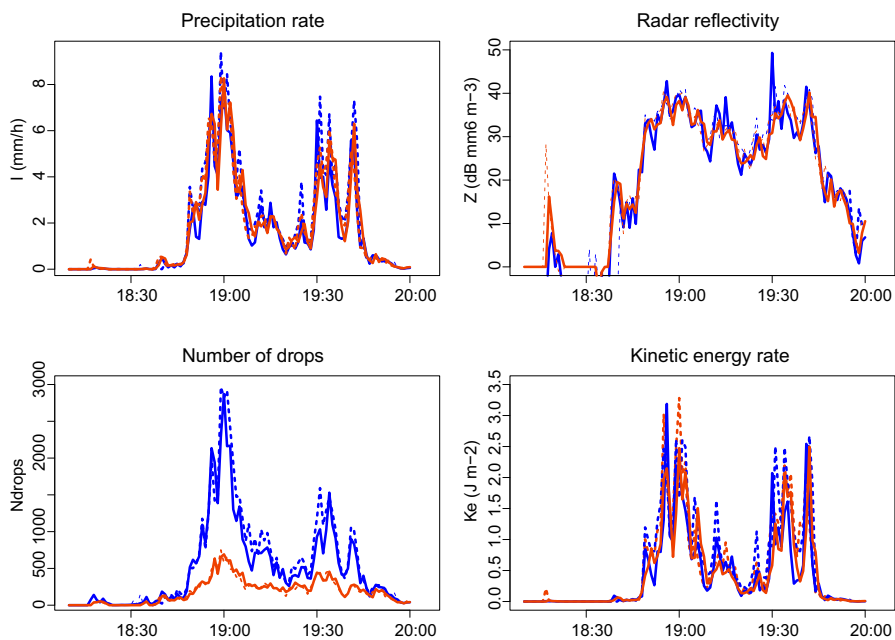


Figure 3. Bulk variables time series of high and low intensity events. Thies in blue and PARSIVEL in red.

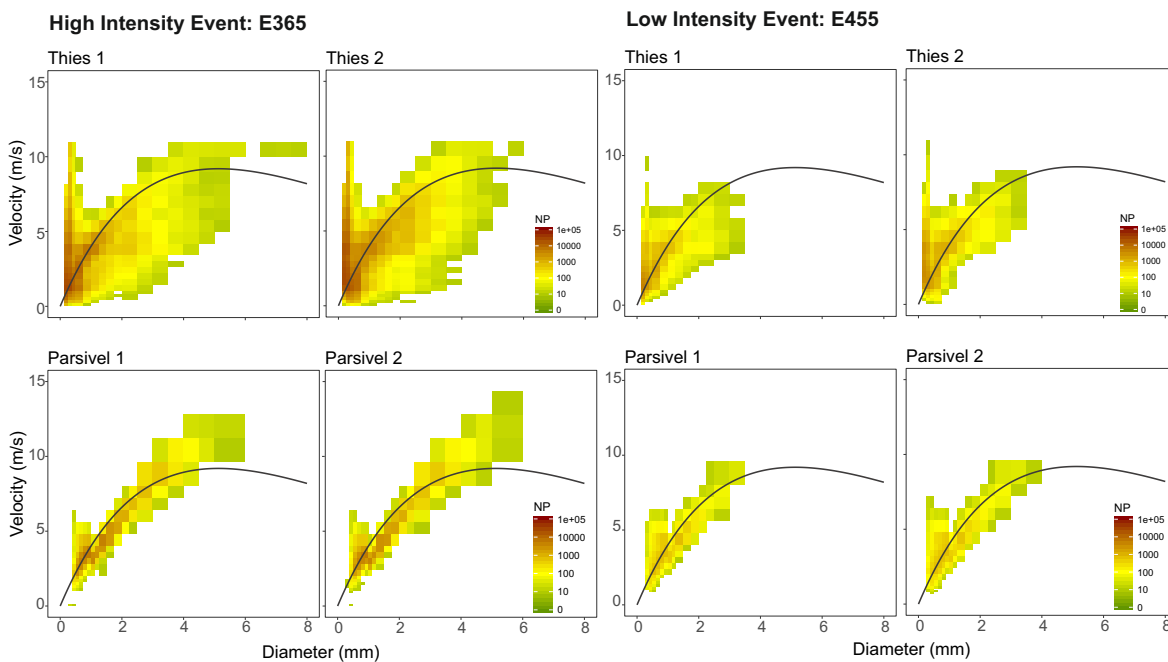


Figure 4. Particle size and velocity density (PSVD) plot of high and low intensity events. Drop size- terminal velocity relationship (Uplinger, 1981) is shown by the black line.

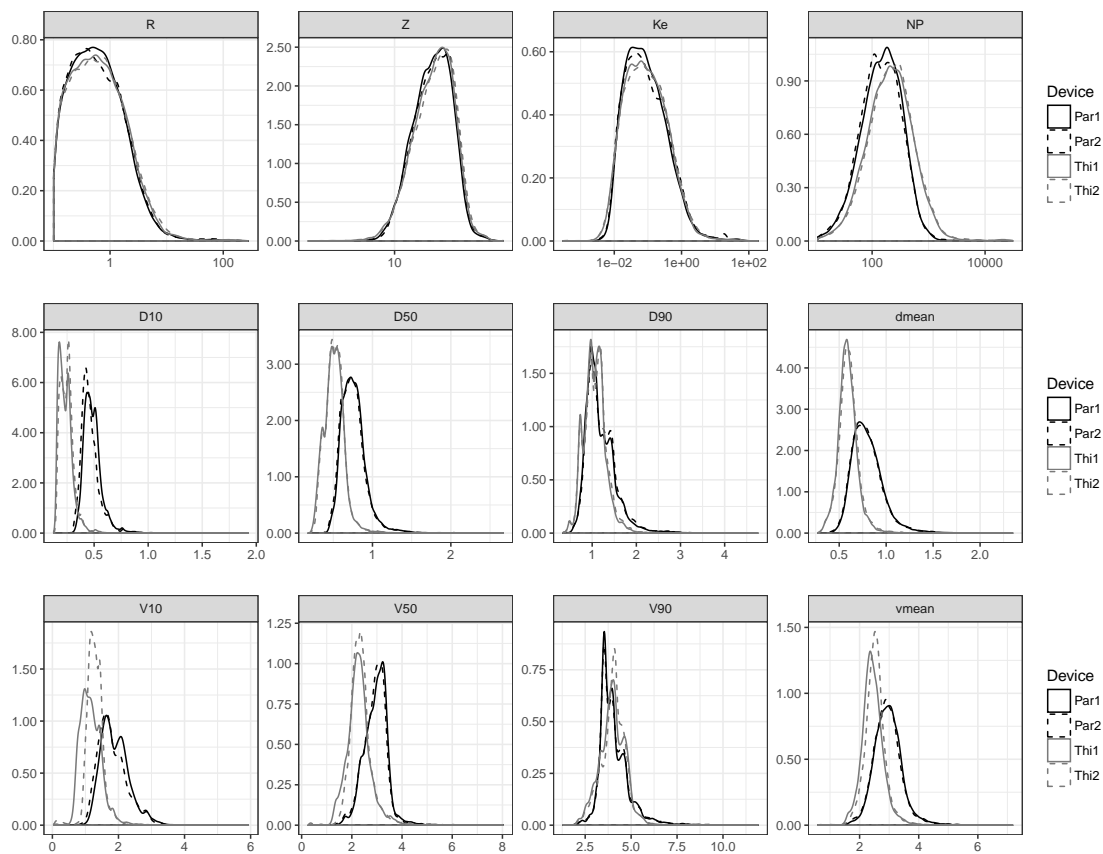


Figure 5. Kernel density plots for one-minute records

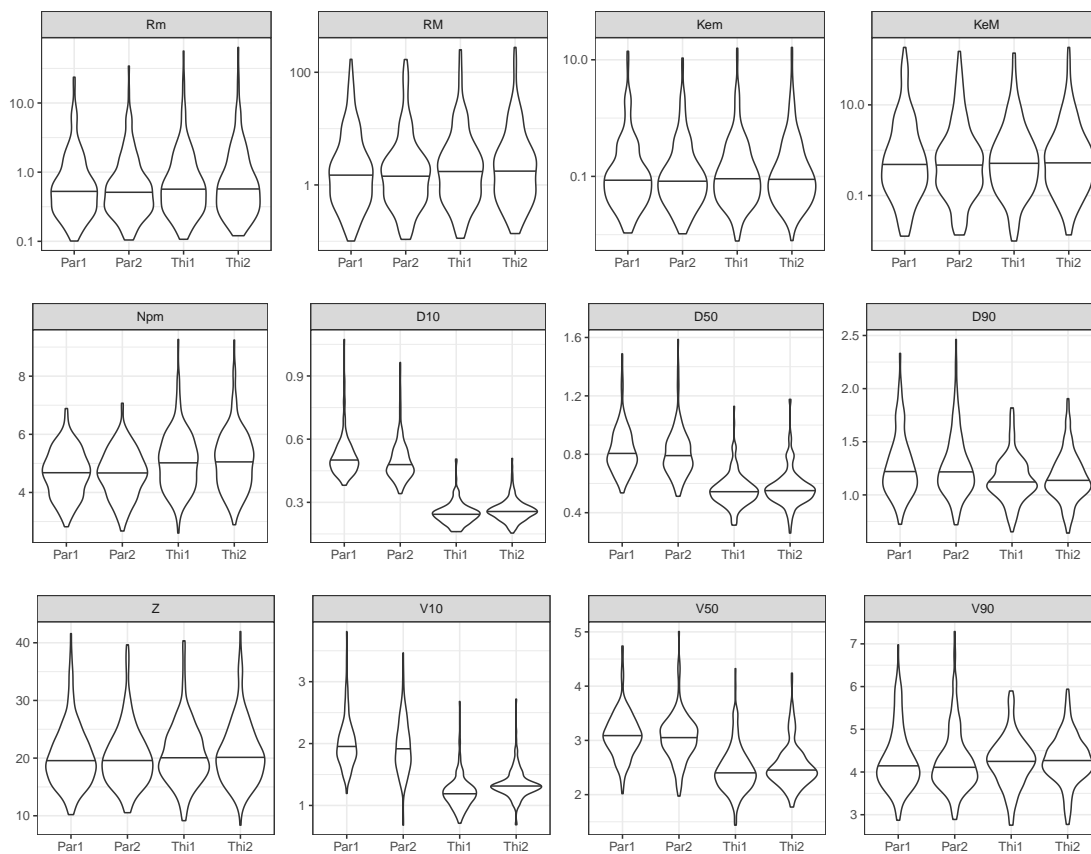


Figure 6. Violin plots for events totals



Appendix A: Additional figures

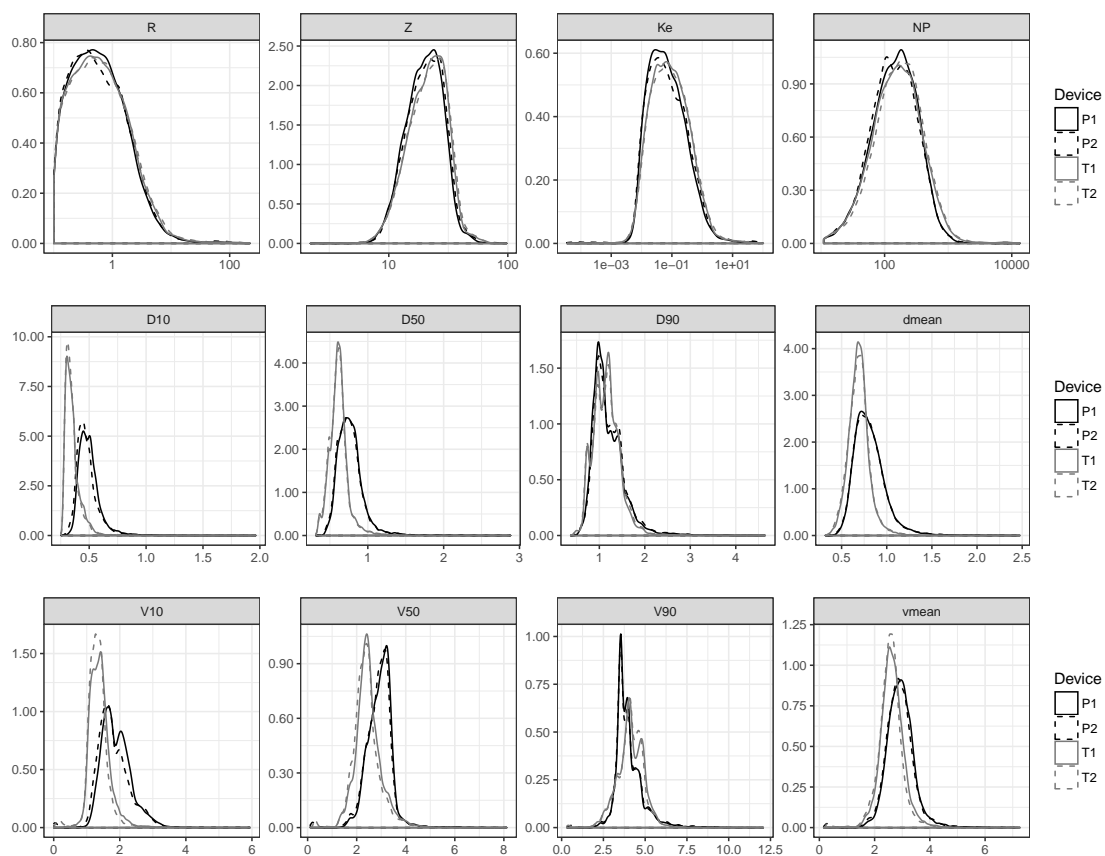


Figure A.1. Kernel density plots for filtered one-minute records

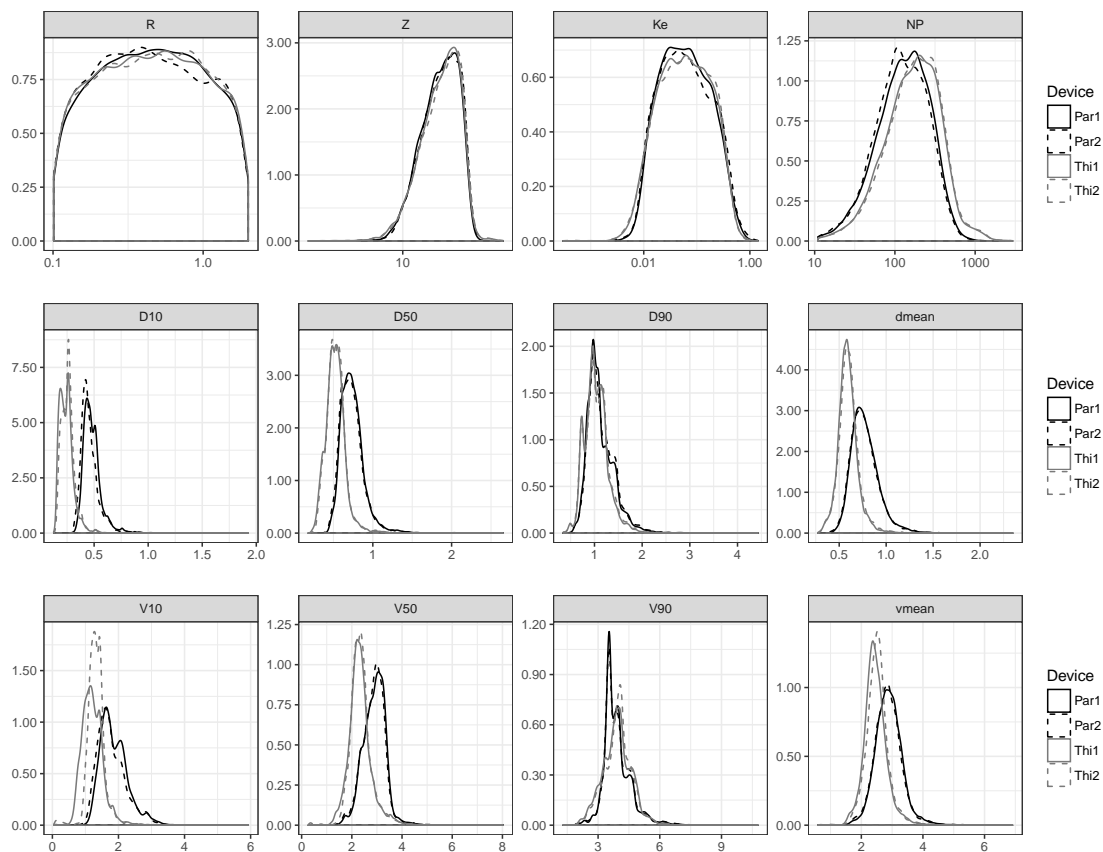


Figure A.2. Kernel density plots for low rainfall intensities ($0.1 < I < 2 \text{ mm h}^{-1}$)

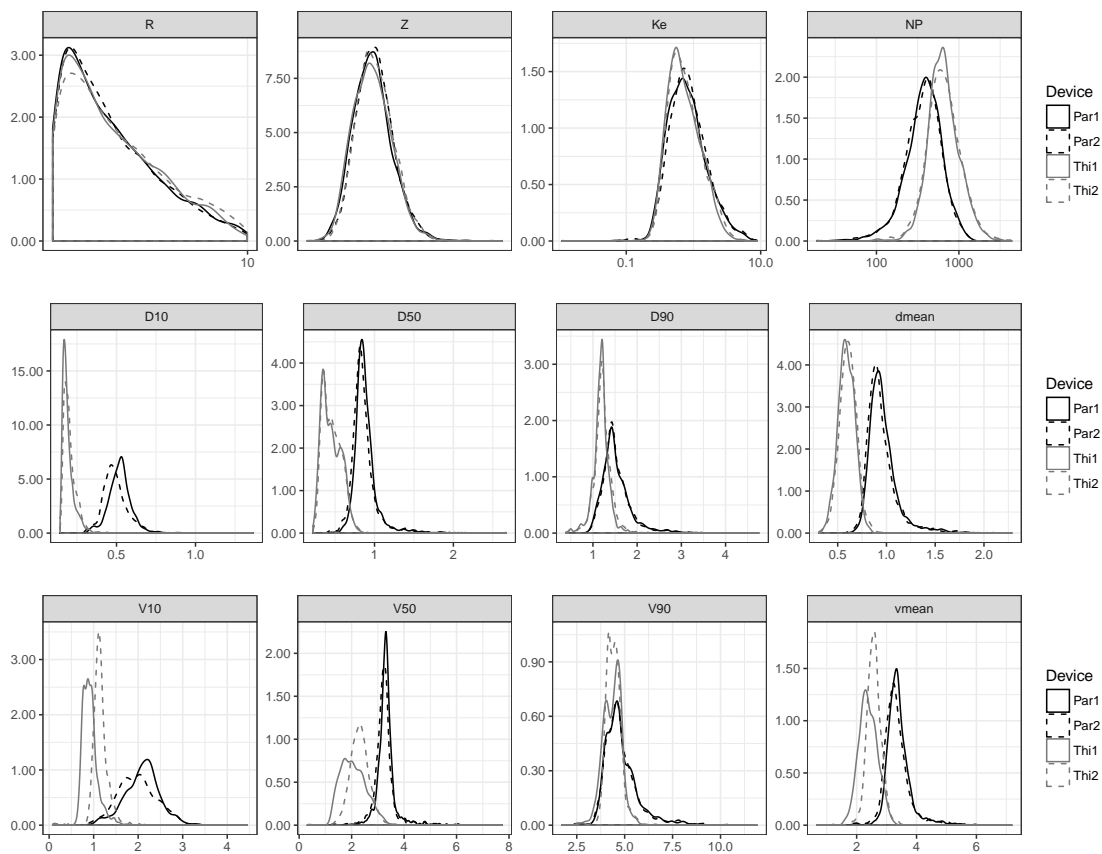


Figure A.3. Kernel density plots for rainfall intensities ($2 < I < 10 \text{ mm h}^{-1}$)

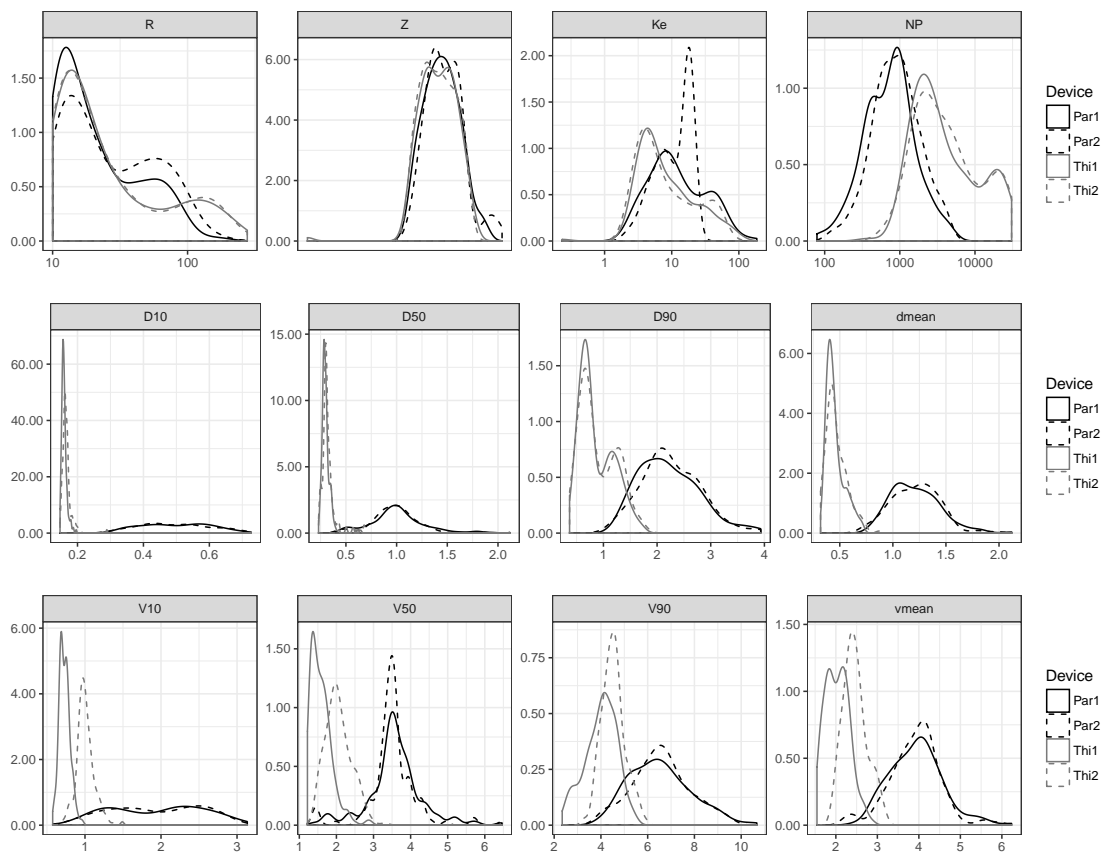


Figure A.4. Kernel density plots for rainfall intensities ($I > 10 \text{ mm h}^{-1}$)

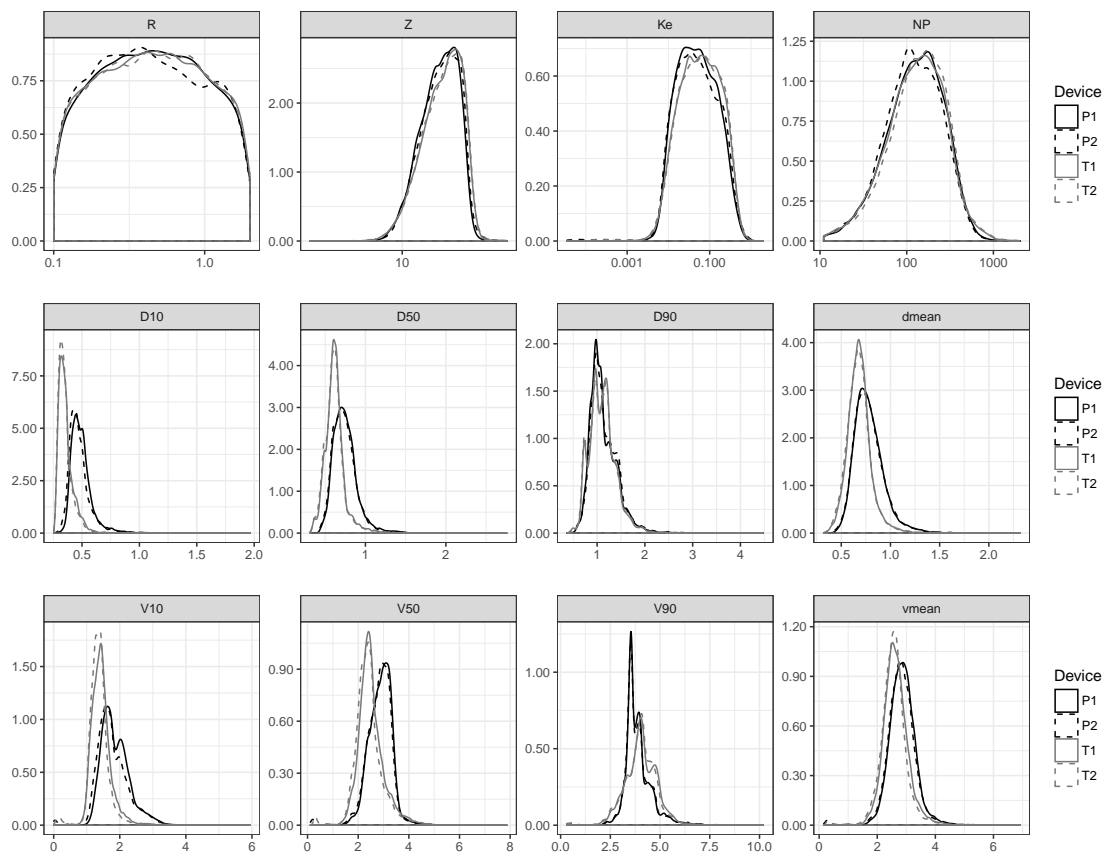


Figure A.5. Filtered kernel density plots for low rainfall intensities ($0.1 < I < 2 \text{ mm h}^{-1}$)

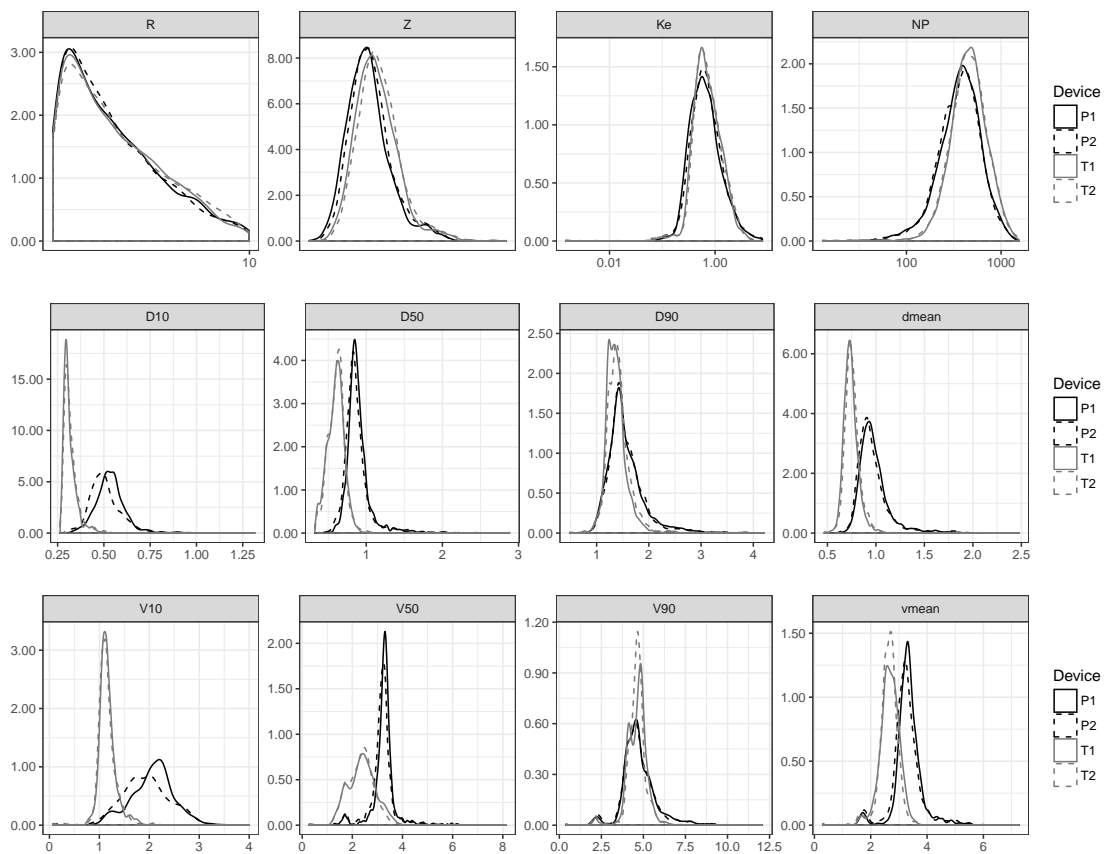


Figure A.6. Filtered density plots for rainfall intensities ($2 < I < 10 \text{ mm h}^{-1}$)

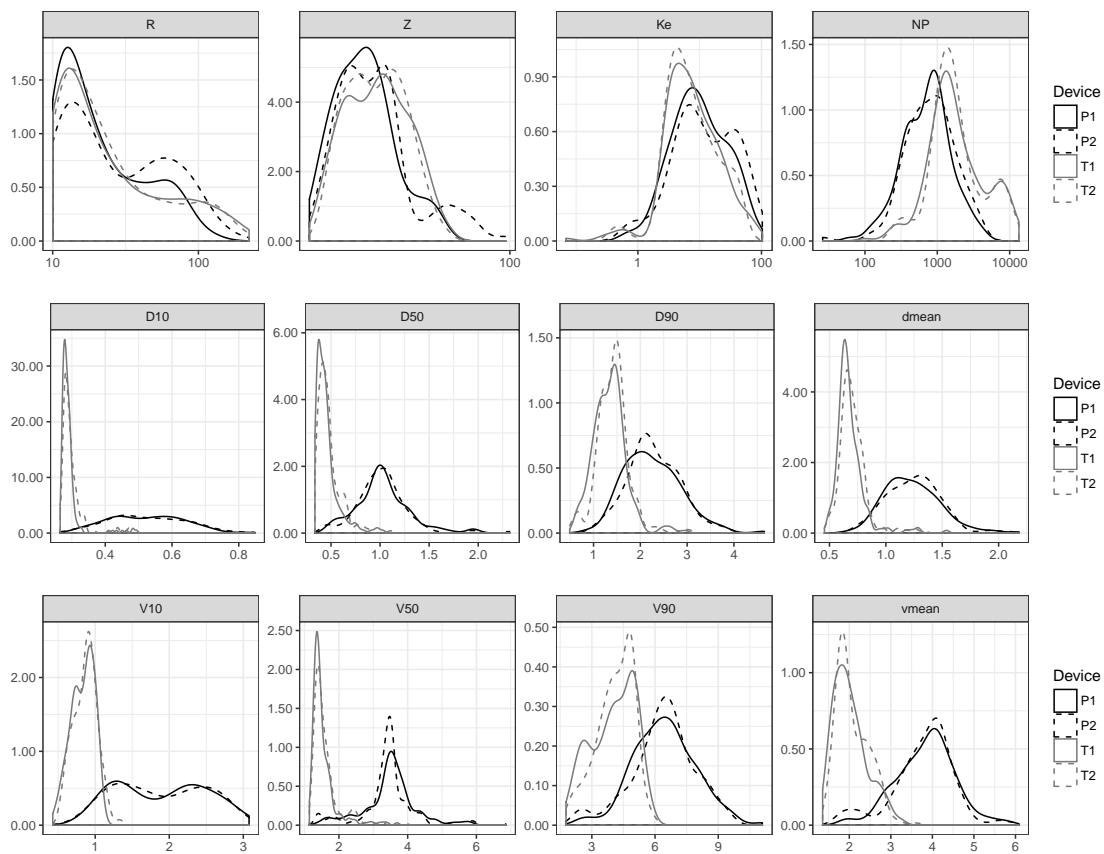


Figure A.7. Filtered density plots for rainfall intensities ($I > 10 \text{ mm h}^{-1}$)